

High load vortex oscillations developed in Francis turbines

D. Rodriguez¹, A. Rivetti¹, C. Lucino¹

¹Laboratory of Hydromechanics, National University of La Plata, La Plata, Argentina

E-mail: daniel.amancio.rod@gmail.com

Abstract. Francis turbines operating at high load conditions produce a typical flow pattern in the draft tube cone characterized by the presence of an axisymmetric central vortex. This central cavity could become unstable, generating synchronic pressure pulsations, usually called self-excited oscillations, which propagate into the whole machine.

The on-set and size of the central vortex cavity depend on the geometry of the runner and draft tube and on the operating point as well. Numerical flow simulations and model tests allow for the characterization of the different flow patterns induced by each particular Francis turbine design and, when studied in combination with the hydraulic system, including the intake and penstock, could predict the prototype hydraulic behavior for the complete operation zone.

The present work focuses the CFD simulation on the development and dynamic behavior of the central axisymmetric vortex for a medium-head Francis turbine operating at high load conditions. The CFD simulations are based in two-phase transient calculations. Oscillation frequencies against its cavity volume development were obtained and good correlation was found with experimental results.

1. Introduction

Francis turbines operating at off design conditions produce different types of vortices and cavitation which are prone to generate pressure pulsations and vibrations. Some types of vortices can normally be avoided, like the inlet edge suction side cavitation or the von Karman and high partial load vortices, but others like the partial load and high load vortices, can only be minimized in relation to their unfavorable pressure pulsation occurrence.

In particular, the high load vortex has a self-excited nature and could produce hydraulic pressure oscillations due to resonances with the surrounding hydraulic systems as was reported in prototypes [1, 2, 5].

The Francis turbines operating at high load typically presents an axisymmetric vortex located in the draft tube cone centered at the outlet runner crown. Depending on the turbine specific number and runner-draft tube design, this vortex develops different central rotating shapes, from helical types to central axisymmetric cavity volumes.

In general, model tests are performed with a homologous geometry which extends from the inlet spiral case section to the outlet draft tube section, both connected to the Test Rig hydraulic system. This modeled geometries differs from the prototype hydraulic system, which includes the penstock and exit channel among others. From this point of view, model scale measurements of self-excited vortex pressure fluctuations have uncertainty to be scaled up to prototype. Therefore, some hydraulic pressure oscillation calculations have to be made in order to analyze the possibility of high load vortex excitation on prototype, where both cavitation compliance and mass flow gain factor have to be evaluated. Several researchers focus on this regard [3], centered upon the axisymmetric vortex core volume variations for different flows and operational heads.



This work presents a CFD simulations in order to study the central cavity dynamic behavior for different operating points (n_{ED} , Q_{ED}) and boundary conditions. The water vapor cavity development is characterized through two-phase steady-state numerical simulations performed inside the high load vortex operating zone.

For those simulated points where the axisymmetric vortex develops a significant vapor cavity, a time dependent pressure condition was applied at the outlet boundary domain with a transient flow analysis. As a result, the cavity volume oscillations frequency is obtained through the dumped oscillations developed due to a pressure pulse application. This dynamic behavior analysis was complemented with a forced continuous pressure wave, which was applied with different frequencies around the obtained free oscillation frequency value.

The simulated cavity volume behavior is compared to measurements performed in a Francis model test [4, 6].

Additionally, a brief analysis is included related to the vapor cavity volume oscillation frequency as a function of the draft tube fluid domain.

2. CFD simulation characteristics

2.1. Simulated conditions

The simulated points are basically divided in two groups: the two-phase steady state simulations for high load vortex development characterization and the transient two-phase simulations for dynamic analysis purposes. The complete set of analyzed points are included in Table 1.

Table 1. Simulated points. *S: steady state, T: transient, EG: extended draft tube geometry

Point OP#	n_{ED}/n_{EDpeak}	Q_{ED}/Q_{EDpeak}	Analysis Type*	GVO [°]	Vortex development
A	0.93	1.33	S,T, pulse	30	Fully developed
A1	0.93	1.33	T, forced_fn	30	Fully developed
A2	0.93	1.33	T, forced_1.2 fn	30	Fully developed
A3	0.93	1.33	T, forced_0.85 fn	30	Fully developed
A4	0.93	1.33	T, pulse, EG	30	Fully developed
B	1	1.31	S,T, pulse	30	Fully developed
C	1.07	1.28	S,T, pulse	30	Fully developed
C1	1.07	1.28	T, pulse, EG	30	Fully developed
D	1.14	1.26	S	30	incipient
E	1	1.18	S	26	Fully developed
F	1	1.07	S	22	incipient

The dynamic analysis was performed first, by the application of one pressure pulse located at the draft tube outlet section and its corresponding cavity volume free dumped oscillations development (point OP#: A, B and C). On second place and according to the obtained natural frequency, the draft tube outlet section is set-up with a pressure field defined by a forced sinusoidal pressure wave (point OP#: A1, A2 and A3).

In order to visualize the simulated points and its vortex cavity development location, a schematic efficiency hill diagram is represented by the relative speed and discharge factors n_{ED} and Q_{ED} , with the guide vane opening curves (GVO) and the free vortex zone traced on it.

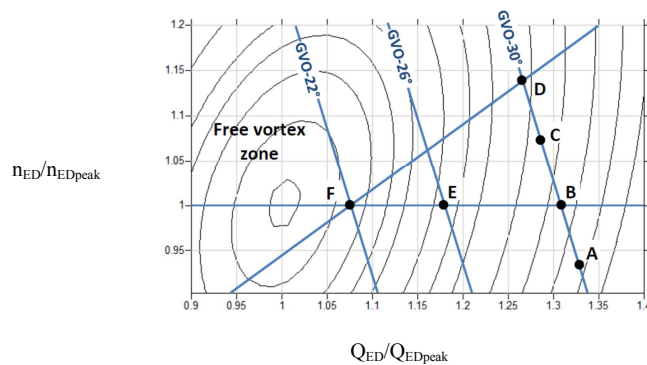


Figure 1. Schematic representation of the efficiency hill diagram and the simulated points location.

2.2. CFD case definition

The numerical simulations were performed using the ANSYS CFX 15.0 software which uses a RANS scheme to solve for the pressure and velocity, modeling turbulence through an extra set of equations. The simulations were performed using the SST model, both in combination with scalable wall functions.

The multiphase configuration was defined by the native CFX cavitation model, where the inter-phase mass transfer between the liquid and vapor phases uses a simplified version of the Rayleigh-Plesset model. The default CFX coefficients and constants were used. For the vapor definition parameters it was used a calorically perfect ideal gas with density variation.

Using periodic boundary conditions, the configuration with model scale includes only one flow channel for the tandem cascade and the runner. The complete draft tube was modeled with an extension at the outlet to avoid disturbances caused by the outlet condition. Also, an extra draft tube extension composed by a volume increment of almost 10 times was applied during dynamic analysis over point OP# A4 and OP#C1.

The meshes were made using ICEM CFD. The tandem cascade was meshed with Tetra/Prism elements and the runner, draft tube and extension with hexa-elements. The complete mesh includes 4.5×10^5 nodes, of which 3.4×10^5 nodes are used in the draft tube. The mesh and the complete configuration are shown in Fig.2.

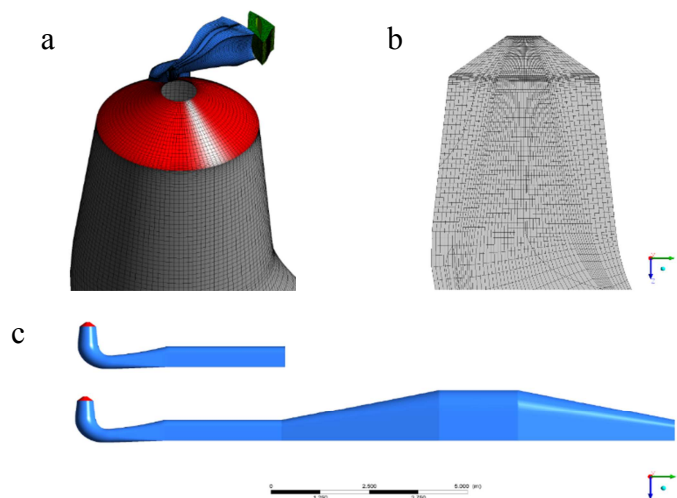


Figure 2. a) Domain discretization for the guide vane, runner and draft tube, model scale. b) Sectional view of the mesh for the vortex core region c) Draft tube domain with and without the extra extension.

For the dynamic response analysis, the transient simulations were performed with 0.002 s (7° runner rotation) and 0.7° runner rotation (Courant number < 1) for dynamic behavior verification. The oscillation frequency differs in 5% between the two transient set-up conditions. For this reason a 7° runner rotation was considered acceptable and adopted in this work.

For those frequency response simulations, it was defined a pressure pulse variation during the run and also an oscillating pressure expression defined by a sinusoidal function.

3. Results and discussion

3.1. Steady state simulations

The high load vortex represented by its axisymmetric cavity volume development is showed for different operating points, from incipient to fully developed condition. The first series, was simulated for constant GVO varying the runner speed and flow in order to obtain the appropriate head. The exit pressure level was set according to Sigma considerations. Figure 3 shows pressure fields and cavity volume iso-surfaces for water vapor volume fraction defined by 0.5 in steady state simulated points OP#: A, B, C and D.

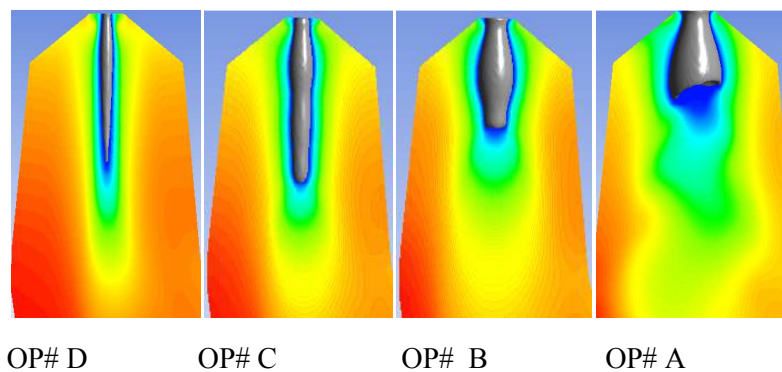


Figure 3. Representation of pressure fields and water vapour cavity volumes (2-Phase) for constant GVO (30°) varying speed factor n_{ED} .

Operation points D, C and B, remains with axisymmetric flow field in the whole draft tube cone, only the last part of the vortex is located at the draft tube elbow entrance, and has sporadic helical shape according to model test observations, [4]. This lack of representation, could be due to the SST adopted model and the central core discretization refinement. However, and taking into account that the main objective was to represent the axisymmetric part of the vortex for water vapour cavity frequency oscillations, the obtained cavity shapes represent accordingly the Francis high load vortex development.

Following with the other results, points A and B present a fully developed cavity where normally synchronic pressure oscillations arise and instabilities occurs at model tests.

Point OP# B, located at n_{ED} close to the corresponding hill diagram peak efficiency, also has an helical final part of the vortex, which is not represented in the picture.

At operation point OP# A, clearly the cavity volume is enhanced and shows a sharp difference from the axisymmetric flow pattern and the helical vortex behavior. At this point, with the maximum simulated water vapor cavity volume, several transient simulations were performed in order to capture synchronic oscillations.

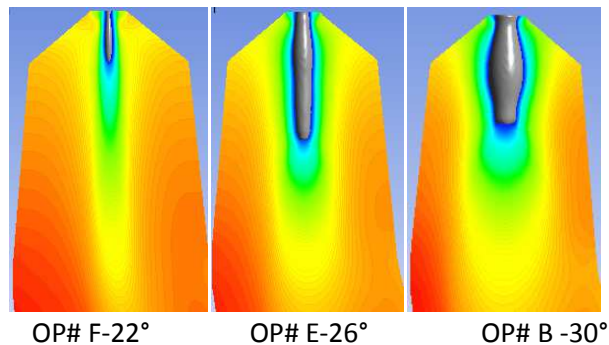


Figure 4. Representation of pressure fields and water vapour cavity volumes (2-Phase) for constant speed factor n_{ED} , varying GVO [$^{\circ}$].

Another CFD sequence was simulated for constant n_{ED} corresponding to peak efficiency and varying GVO, as could be seen on figure 4. OP# F shows an incipient vortex. In conjunction with OP# D, it permits to draw the beginning of the high load vortex curve, which limits the free vortex zone in the efficiency hill diagram. On figure 5 could be compared the CFD simulations from OP#B to OP#F, for n_{EDpeak} . According to Q_{ED}/Q_{EDpeak} , picture #6 correspond approximately to OP#B and #2 with OP#E.

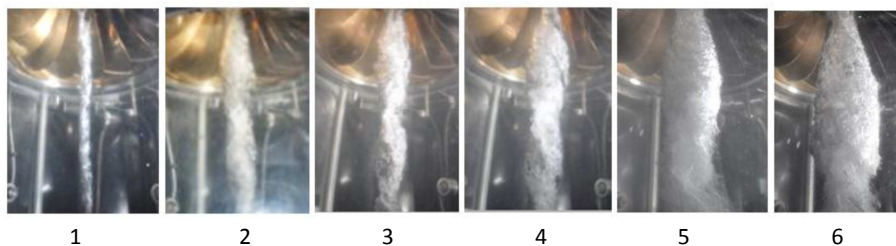


Figure 5. Vortex visualization equidistant sequence for: n_{EDpeak} from $Q_{ED}/Q_{EDpeak} = 1.14$ to 1.31. Results reported in Rodriguez D.et.al [4].

As a general remark, the high load vortex 2-phase SST simulation captures the water vapor cavity development acceptably for the axisymmetric part of the vortex located in the draft tube cone. Differences arise in the last part of the vortex, where the cavity adopts a sporadic helical shape, mainly on OP# B.

3.2. Frequency analysis of the water vapor cavity oscillations

In order to get a better understanding of the water vapor cavity oscillations frequency, a series of transient 2-phase SST simulations, based on the previous calculations, were developed. For that purpose, the steady state simulations were used as the initial condition for the transient CFD calculations. Three points were simulated, OP# A, B and C, obtaining the free water vapor cavity dumped oscillation on each one due to a pressure pulse application at the extended draft tube outlet section.

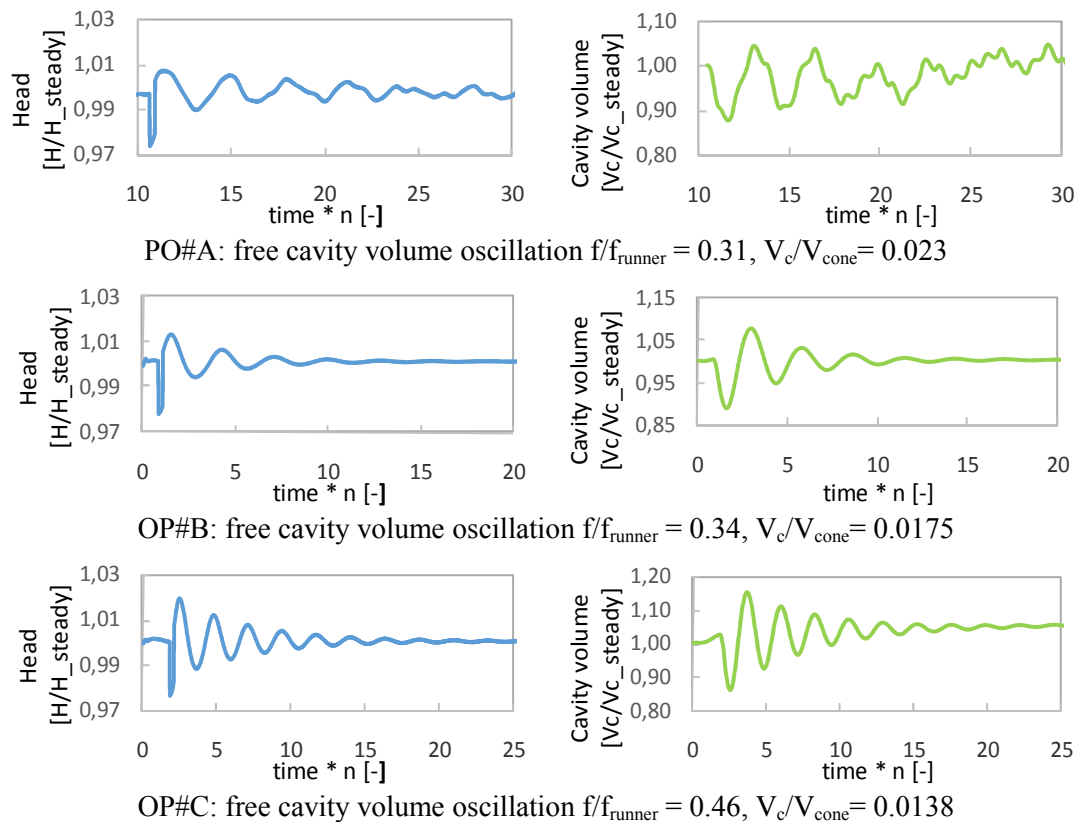


Figure 6. Left: pressure pulse applied during transient run. Right: damped cavity volume oscillations due to pressure pulse application as a function of runner rotations.

Analysis of the cavity volume response due to the pressure pulse application, allows us to know the natural oscillation frequency for the simulated domain.

As observed in the three simulated conditions, OP# A, B and C, the cavity oscillations frequency has a dependency with the cavity volume. An increment in the cavity volume produces a decreasing cavity oscillation frequency.

Although the oscillations showed in figure 6 are not self-sustained, model tests [4] present instabilities with synchronic pressure pulsations on OP#A and OP#B. Thus, the simulated fluid domain and SST applied model is not capturing the self-induced instabilities. However, the objective related to analyze the oscillation frequency as a function of the cavity volume development could be described.

Complementary, on OP#A, where the volume cavity reaches an important volume, it was applied a forced pressure field with a time domain sinusoidal function for three different frequencies, below, equal and above the natural obtained frequency. The applied forced excitation amplitude was 0.1% of the head.

When the excitation frequency is 1.2 times the natural frequency (f_n), the volume amplitude reaches 30% peak to peak value from the amplitude excited at resonance frequency. Similar behavior is obtained with excitation frequency below f_n , applying $0.85 f_n$, the cavity volume increment is 40% peak to peak. In some way, the different cavity volume oscillation amplitudes obtained due to forced frequency variations, confirm that an amplification effect is produced when the excitation is applied close to natural frequency.

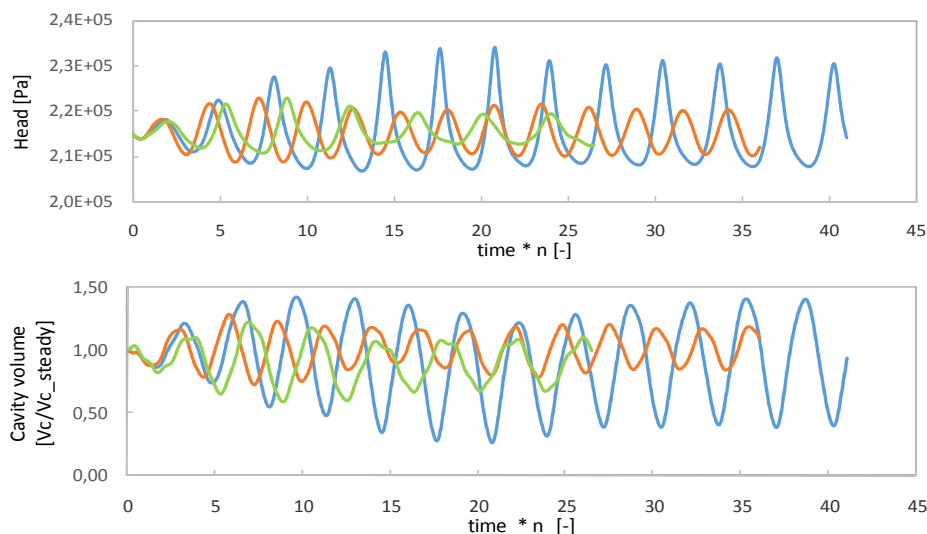


Figure 7. Top: pressure oscillation. Bottom: water vapour cavity volume oscillation. Blue curve: due to sinusoidal pressure field excitation at natural frequency f_n . Red curve correspond to $1.2 f_n$ and green curve to $0.8 f_n$.

The cavity volume oscillation represented in figure 7 due to f_n pressure excitation, can be followed in figure 8 where a half cycle shows five equidistant time steps from minimum to maximum cavity volume development.

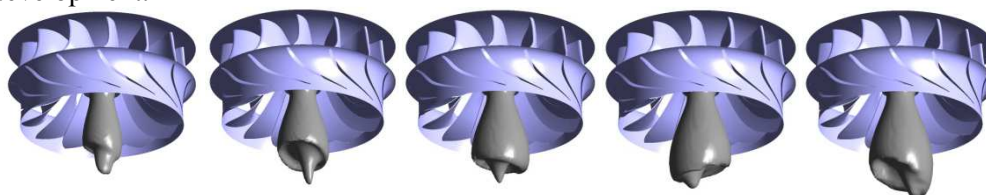


Figure 8. OP#A, excited with a forced sinusoidal pressure field at natural frequency. Water vapour cavity volume oscillation from peak to peak, half cycle. Iso-surface vapour volume fraction 0.5.

Another cavity oscillation study was performed on OP#A4 and OP#C1 with a different draft tube domain. The draft tube geometry was extended with an added fluid volume of 10 times compared with the previous calculations. The absolute pressure was adjusted in order to get the same cavity volume as in the previous run. With this extended geometry, a pressure pulse was applied obtaining a decreasing value in the free oscillation cavity frequency of 12% and 25% respectively. More studies have to be performed in order to define the most appropriate fluid domain to be considered in the simulations.

3.3. Discussion

The cavity oscillation frequency obtained by CFD simulation has shown a strong dependence with the axisymmetric vapor volume itself. For increasing cavity volume developments a decreasing frequency occurs.

On the other hand, the natural frequency is also determined by the simulated fluid domain. An increasing fluid domain produces a decreasing frequency response for the same cavity volume development.

Those results could be represented by a power law regression curve. On figure 9, the CFD results are complemented with physical simulations performed by different authors and testing facilities. The

frequencies and cavity volumes are normalized by the runner rotation frequency (f_{runner}) and the draft tube cone volume (V_{cone}) respectively.

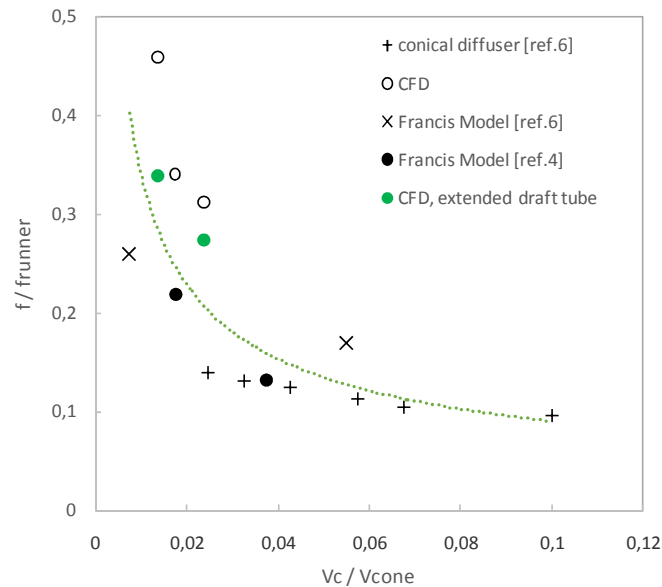


Figure 9. Central vortex oscillation frequencies vs vapor cavity volume. The power law regression curve includes de CFD results (Francis $nq=47$) with extended draft tube and the physical simulations (+ conical diffuser, \times Francis $nq=42$ and \bullet Francis $nq=49$).

The analysis of the oscillation frequency as a function of the cavity volume change allows us to discuss some aspects related to the high load vortex pressure fluctuations at different project stages. One aspect, at early design stage, is related to the verification of the hydraulic system (penstock-turbine) against vibrations eigenmodes and standing waves, both in relation to the oscillation frequencies of the vortex cavity. Another aspect could be linked with the mitigation strategy due to instabilities that occur on the prototype.

Regarding the study of eigenfrequencies and standing pressure waves for the penstock-turbine system, commonly, the frequency analysis includes the partial load vortex excitation frequency ($0.25 \cdot f_{\text{runner}}$). If it is also taken into account the high load self-excited vortex frequencies, we can define two cases according to the runner design and its particular vortex development and operation zone.

In one case, if the runner-draft tube design presents in the high load region an axisymmetric central vortex cavity volume $V_c / V_{\text{cone}} > 0.02$, its instability frequencies will be below the partial load frequency.

On the other hand, if the runner design develops at high load an axisymmetric vortex volume below $V_c / V_{\text{cone}} < 0.02$, the possible cavity oscillation frequency will exceed the partial load frequency. In this case and as was reported by Muller [6], the amplitude of the pressure fluctuations are substantially less than the fluctuations due to fully developed cavities with $V_c / V_{\text{cone}} > 0.02$.

If we now analyze the prototype behavior, the possible strategies for mitigating pressure oscillations at high load operation could include different options, for example, geometrical changes in the original design and air incorporation [5]. In every case it is important to know the vortex volume development (V_c / V_{cone}).

Taking into account the frequency- cavity volume power law regression curve, we can see that for highly developed vortices, any attempt to change the vortex volume involves small changes in the oscillation frequency. Conversely, for small vortices, slight volume increments produces important frequency variations.

4. Conclusion

This work has studied the behavior of a Francis turbine operating under high load conditions where an axisymmetric vortex core develops. The steady state 2-phase simulations have shown the high load vortex development for different operating points. The 2-phase transient simulations have allowed the water vapor cavity volume frequency calculations in order to evaluate the dynamic behavior of the high load self-excited hydraulic oscillations.

The CFD simulations have been correlated with good agreement against physical model results describing the cavity oscillation frequency in relation with the vortex volume.

Depending on the cavity volume development, two distinct behaviors were analyzed for V_c/V_{cone} : below and above 0.02. At this value, the high load vortex oscillation frequency is similar to that corresponding to the partial load vortex frequency.

In the case of $V_c/V_{cone} < 0.02$, for big cavity volumes, the vortex may oscillate with frequencies below $0.25 \cdot f_{runner}$, and for small cavity volumes, the instabilities could arise above this value.

Indeed, at each situation, the frequency-cavity volume rate is different: if we have instabilities caused by $V_c/V_{cone} > 0.02$, slight frequency changes are insinuated due to a vortex volume variation. Contrary to that, for incipient to medium vortex developments, an important frequency variation is produced from small cavity volume changes.

References

- [1] Arzola F et al. 2006 Undesired Power Oscillations at High Load in Large Francis Turbines Experimental Study and Solution, IAHR 23rd Symp. on Hydraulic Machinery Systems (Yokohama, Japan)
- [2] Koutník J et al. 2006 Overload surge event in a pumped storage power plant IAHR 23rd Symp. on Hydraulic Machinery Systems (Yokohama, Japan)
- [3] Dörfler, P K et al. 2010 Francis full-load surge mechanism identified by unsteady 2-phase CFD IAHR 25th Symposium on Hydraulic Machinery Systems (Timișoara, Romania)
- [4] Rodriguez D, Rojido M, Cacciavillani C. 2015 Francis turbine operating at high load- Model scale flow analysis. IAHR Latin American Meeting, La Plata, Argentina.
- [5] Dörfler, P. 2012 Flow-Induced Pulsation and Vibration in Hydraulic Machinery. Springer. pp 140,141,203-207.
- [6] Müller Andres. 2014 *Physical Mechanisms governing Self-Excited Pressure Oscillations in Francis Turbines*, PhD thesis, EPFL, Lausanne, Switzerland.